1      <u>**Revision 1**</u>

2  # A simple method for obtaining heat capacity coefficients of
3  # minerals

4      Total word count: 4325, Main body word count: 2005

5      Samuel Bowman*, Arkajyoti Pathak, Vikas Agrawal, and Shikha Sharma

6      Department of Geology and Geography, West Virginia University, Morgantown, WV 26506

7      *Samuel Bowman, G-29 Brooks Hall, 98 Beechurst Ave, Department of Geology and Geography, West
8      Virginia University, Morgantown WV, 26506, sabowman@mix.wvu.edu

9      _____

10     # Abstract

11     Heat capacity data are unavailable or incomplete for many minerals at geologically relevant

12     temperatures.  Despite the availability of entropy and enthalpy values in numerous thermodynamic

13     tables (even sometimes at elevated temperatures), there remains  need forextrapolation beyond or

14     interpolation between temperatures.  This approach inevitably results in estimates for entropy and

15     enthalpy values because the heat capacity coefficients required for optimal thermodynamic

16     treatment are less frequently available.  Here we propose  a simple method for obtaining heat

17     capacity coefficients of minerals.  This method requires only the empirically measured temperature-

18     specific heat capacity for calculation via a matrix algorithm.  The system of equations solver is written

19     in the Python computing language and has been made accessible in an online  repository.

20     Thermodynamically, the solution to a system of equations represents the heat capacity coefficients

21     that satisfy the mineral-specific polynomial.  Direct coefficient calculation will result in more robust

22     thermodynamic data which is not subject to fitting uncertainties.  Using hematite as an example, this

23     method provides results which are comparable to conventional means and is applicable to any solid

24     material.  Coefficients vary within the traditional large 950 K temperature interval, indicating that

25     best results should instead utilize a smaller 400 K temperature interval.  Examples of large-scale

26    implications include refinement of geothermal gradient estimation in rapidly subsiding sedimentary

27    basins, or metamorphic or hydrothermal evolution.

28    Keywords: Gaussian elimination, heat capacity, hematite, system of equations

# Introduction

30        Earth systems are rarely, if ever, truly at standard temperature and pressure, the

31    effect of these parameters must be considered for robust thermodynamic treatment.

32    Regarding systems at non-standard temperatures, mineralogists and petrologists employ

33    (directly or indirectly) the heat capacity ($C_P$) for the selected material(s) for purposes such

34    as studying the effects of temperature and pressure for basin modeling or maturity modeling

35    (Waples and Waples, 2004).  However, despite the wide availability of $C_P$ data for many

36    minerals, in most cases, the numbers are often applicable to narrow temperature ranges.  In

37    other cases, the entropy ($\Delta S$) and enthalpy ($\Delta H$) must either be extrapolated or interpolated

38    to the desired temperature (Robie and Hemingway, 1995), or the final free energy ($\Delta G_f$) is

39    obtained via linear regression (Toulmin and Barton, 1964). Considering that $C_P$ follows a

40    polynomial trend for temperature, it is expected that linear regressions of free energy may

41    introduce uncertainty (although linear behavior may provide reasonable estimates for free

42    energy using small $\Delta T$ intervals).  One limitation within the present heat capacity literature

43    may be found for the mineral hematite in Hemingway (1990), where there is a function

44    discontinuity occurring at 950 K; between the lower (T<950 K) and upper (T>950 K)

45    temperature domains.  The heat capacity of a solid is typically continuous except for

46    occasional discontinuities and has been attributed to crystallographic/phase transitions

47    (e.g., Guyot et al., 1993).  Heat capacity function discontinuities will be translated to the

48    calculated or regressed polynomial coefficients.  Ideally, the characteristic mineral specific

49    $C_P$ coefficients have been determined and published, allowing for exact calculation of entropy

50    and enthalpy at a given temperature.  Unfortunately, these coefficients are often unavailable

51    throughout the literature, one notable exception being the compilation in Robie and

52    Hemingway (1995).

53        Fundamentally, the heat capacity of a material is effectively the input energy required

54    to raise the thermal energy of that same material.  The heat capacity is vital to mineralogical,

55    petrological, and geochemical research.  It is quantified for a selected material using various

56    calorimetric techniques and when plotted against temperature, takes the form of a

57    polynomial (e.g., Klemme and van Miltenburg, 2003; Benisek et al., 2012).  The $C_P$ polynomial

58    order and the number of coefficients varies throughout the literature.  For example, the form

59    in Xiong et al. (2016) contains seven coefficients and is a third-order polynomial, while the

60    Shomate equation (e.g., NIST) has five coefficients and is also a third-order polynomial, while

61    the progenitor, the Maier-Kelley form contains only three coefficients and is a second order

62    polynomial (Maier and Kelley, 1932).  The form commonly found associated with geological

63    solids or minerals is the second order polynomial with five coefficients as given by

64    Hemingway et al. (1978).  Finally, the $C_P$ polynomial formula is often determined by

65    regression of existing data to fit aspecific polynomial form (Hemingway, 1990; Waples and

66    Waples, 2004).  The primary goal of this study is to evaluate the polynomial through direct

67    means. This approach allows for smaller ΔT to be utilized and eliminates any introduced

68    fitting bias (e.g., overfitting) (Gamsjäger and Wiessner, 2018).  Therefore, employing this

69    direct coefficient calculation technique relies solely upon the empirical $C_P$, ensuring that the

70    polynomial retains fidelity.  In other words, as the direct calculation is axiomatically correct,

71    the values obtained from the equation proposed in this contribution will remove much of the

72    errors associated with measurements from interpolated and extrapolated values available

73    in the literature so far.  Finally, this method can be used to directly calculate thermal

74    diffusivity, a crucial physical parameter of geological systems that reflects the ability to

75    conduct thermal energy relative to its ability to store the energy (Fuchs et al., 2021).

76    Applications of accurate heat capacity measurement are in the fields of geothermal gradient

77    determination in active basins, basin modelling and studying geodynamic transformations

78    in tectonically active regions.

# Methodology

79

## Theoretical Background

80

81          Here, we offer a simple method for the determination of the characteristic coefficients

82    requiring only a suite of five $C_P$ values at their corresponding temperatures.  For solids, the

83    relationship between heat capacity and temperature is non-linear (e.g., Robie et al., 1978;

84    Klemme and van Miltenburg, 2003; Benisek et al., 2012; Xiong et al., 2016; Ulian et al., 2020;

85    Vassiliev and Taldrik, 2021), implying that linear determination of $\Delta G_f$ is likely to induce

86    uncertainty of over(under)estimation compared to a polynomial fit.  For a $C_P$ equation with

87    five coefficients, there are five vectors-each at five unique temperatures with accompanying

88    scalars.  Note that the scalars are equal to the coefficients (which of course are the same for

89    all vectors (i.e., all temperatures)).  The intersection of the vectors is the solution to the

90    system of equations, where there are an equal number of scalar coefficients which satisfy all

91    $C_P$ equations at each temperature simultaneously.  Once the scalar coefficients have been

92    evaluated, $\Delta S, \Delta H,$ and ultimately $\Delta G_f$ at a selected temperature may be determined.

93          For a $C_P$ polynomial with n equations and n coefficients, there is a square n*n matrix,

94    written in the general form $\mathbf{A}x=\mathbf{b}$, or

95
$$\begin{bmatrix} a_{11} & \cdots & a_{1n} \\ \vdots & \ddots & \vdots \\ a_{n1} & \cdots & a_{nn} \end{bmatrix} * \begin{bmatrix} x \\ \vdots \\ x_n \end{bmatrix} = \begin{bmatrix} b \\ \vdots \\ b_n \end{bmatrix}.$$
  EQ.1

96   This method may be employed for any solid substance in which existing $C_P$ data is known at

97   a corresponding temperature.  As an illustrative example calculation, let us consider an

98   example for hematite using $C_P$ polynomial found in Hemingway (1990), where

99   $C_P = A - BT + CT^2 - DT^{-0.5} + ET^{-2}.$   EQ.2

100   This form has five coefficients and is a second-order polynomial.  Now, for an n x n matrix,

101   there are five reported $C_P$ at five temperatures requiring five equations.  Combining the $C_P$

102   polynomial with EQ.1, **A**x=**b** becomes (approximately)

103
$$\begin{bmatrix} 1 & 400 & 1.6E+5 & 0.050 & 8.25E-6 \\ 1 & 500 & 2.5E+5 & 0.045 & 4.00E-6 \\ 1 & 600 & 3.6E+5 & 0.041 & 2.78E-6 \\ 1 & 700 & 4.9E+5 & 0.038 & 2.04E-6 \\ 1 & 800 & 6.4E+5 & 0.035 & 1.56E-6 \end{bmatrix} * \begin{bmatrix} x_1 \\ x_2 \\ x_3 \\ x_4 \\ x_5 \end{bmatrix} = \begin{bmatrix} 120.91 \\ 131.39 \\ 139.01 \\ 146.53 \\ 156.06 \end{bmatrix}.$$
  EQ.3

104   Note that **b** to the right of the equals sign in EQ.3 contains the temperature-specific $C_P$ in

105   Hemingway (1990 from 400 to 800 K.  The coefficients are obtained through Gaussian

106   elimination and by taking the augmented matrix to reduced row echelon form (rref) via

107   elementary row operations.  Rewriting, we find the augmented matrix becomes **A|b**

108
$$\begin{bmatrix} 1 & 400 & 1.6E+5 & 0.050 & 8.25E-6 & 120.91 \\ 1 & 500 & 2.5E+5 & 0.045 & 4.00E-6 & 131.39 \\ 1 & 600 & 3.6E+5 & 0.041 & 2.78E-6 & 139.01 \\ 1 & 700 & 4.9E+5 & 0.038 & 2.04E-6 & 146.53 \\ 1 & 800 & 6.4E+5 & 0.035 & 1.56E-6 & 156.06 \end{bmatrix} \xrightarrow{rref} \begin{bmatrix} 1 & 0 & 0 & 0 & 0 & 994.40 \\ 0 & 1 & 0 & 0 & 0 & -0.78862 \\ 0 & 0 & 1 & 0 & 0 & 3.9574E-4 \\ 0 & 0 & 0 & 1 & 0 & -1.3361E+4 \\ 0 & 0 & 0 & 0 & 1 & 7.4669E+6 \end{bmatrix}.$$
  EQ.4

109   The five coefficients, after the $x_n$ scalar matrix transpose and substitution become

110
$$\begin{bmatrix} x_1 \\ x_2 \\ x_3 \\ x_4 \\ x_5 \end{bmatrix}^T = [A \quad B \quad C \quad D \quad E] = [994.40 \quad -0.78862 \quad 3.9574E-4 \quad -1.3361E+4 \quad 7.4669E+6],$$
  EQ.5

111   where A = $x_1$ and E = $x_5$.  Upon coefficient back-substitution into the $C_P$ polynomial, the

112   empirical $C_P$ is returned at each temperature sub-equation.  One limitation of this approach

113   is that it requires a square n x n matrix, and thus, the number of temperature sub-equations

114   are limited to the number of coefficients in the polynomial.  If there are more temperatures

115   (rows) than coefficients (columns), then **A** cannot be taken to rref, and the system does not

116   have a solution.  It is worth noting, that the accuracy and uncertainty of this method it is of

117   course limited to the quality of the reported $C_P$ input data.

## Software Implementation

119         Manually solving a system of equations by rref is a lengthy process-particularly for

120   non-integer numbers.  To this end, it is advantageous to employ a calculator (e.g., online,

121   computer code, etc.).  We have developed $C_P$ Coefficent Calculator ($C^3$) to calculate the

122   coefficients using the rref method above.  Modifying Python3 code found in Kong et al.

123   (2020), $C^3$ is offered under the MIT license, and is available (along with a README manual)

124   at https://github.com/WVUStableIsotopeLab/CodeswithPython.

# Results and Discussion

126         As an example, hematite $C_P$ coefficients obtained from rref calculation are provided

127   in Table 1 (subinterval #2) and are presented in Figure 1.  These data are computed across

128   two major temperature domains (298.15 to 950 K, and 950 to 1800 K) (Hemingway, 1990).

129   Given the sensitivity of the coefficients, the rref direct-calculated results compare favorably

130   to the hematite values reported by Robie and Hemingway (1995).  For the upper-

131   temperature interval (950 K to 1800 K) our proposed method yields an additional coefficient

132   that is not available, as noted in the existing literature.  Robie and Hemingway (1995)

133   provide a line of best-fit regression coefficients over the range of 298 K to 1800 K for A, B,

134   and C of -808.9, 0.2466, and -8.423E-5, respectively.  This is  compared to the direct

135   calculation method presented here, where five coefficients are calculated over a much more

136   condensed temperature range from 400 K to 800 K, in 100 K increments.  We believe that

137   our approach is likely to be more accurate as the temperature interval is significantly

138   reduced and does not cross any phase transition (e.g., 950 K in Figure 2).  In addition, because

139   the relationship between temperature and $C_p$ is non-linear, the curve-fitting approach is

140   particularly susceptible to extrapolation since the rate of change is not constant (i.e., $d^2y/dx^2$

141   ≠0).  Regarding interpolation, empirical $Cp(T)$ data used in both curve-fitting and direct

142   calculation may be improved by reducing the temperature interval between interpolations.

143   These temperature intervals are often given in 100 K increments (e.g., Robie and

144   Hemingway, 1995).  It is worth mentioning that the direct calculation method is an

145   interpolative approach and, thus, is subject to the quality of the $CP(T)$ data and the

146   temperature increments.  If, for example, the temperature increment was decreased to 50 K,

147   the resulting $CP(T)$ would likely lead to even more accurate coefficients. In this scenario, five

148   coefficients could still be determined but over a tighter temperature interval (400 K, 450 K,

149   500 K, 550 K, and 600 K).

150       One of the most striking observations of the tabulated data is that it may display

151   discontinuous behavior when plotted graphically, particularly at the interface between the

152   low and high-temperature domain intervals (~950 K) (Figure 2).  Moreover, note the change

153   in the concavity between the low and high-temperature domain intervals.  The highest $C_P$

154   value across the entire temperature range is at 950 K, and the significant trough about

155   ~1300 K.  This observation along with the discontinuity at 950 K indicate that the resulting

156   coefficients will be subsequently affected.  Indeed, when temperature intervals of ~400 K

157   are utilized, the coefficients are not static but drift (Table 1).  It is apparent that the most

158   accurate coefficients are those which minimize temperature drift obtained by performing

159    the rref calculation over a small $\Delta T$ interval. Since entropy and enthalpy are produced from

160    integrating $C_P{}^o/T$ and $C_P$ (where $C_P$ is the selected polynomial with commensurate

161    coefficients) over a range starting at 298.15 K, it is reasonable to use, say, for a temperature

162    of 780 K to use coefficients that pertain to a subinterval (i.e., subintervals #2 or #3 in Figure

163    2 and Table 1) instead of conventional coefficients for the entire 298.15 to 950 K domain.

164    For the temperature intervals <950 K, the behavior is relatively linear (subintervals #1 to #4

165    in Figure 2). In comparison, the temperature intervals >950 K are parabolic about the local

166    minimum at ~1300 K. This behavior is translated to the $C_P$ values as well (subinterval #6 in

167    Figure 2 and Table 1).

# Implications

169    The heat capacity is a fundamental aspect not only limited to minerals but also liquids,

170    gases, and dissolved species. It underlies thermodynamics as it is necessary for entropy,

171    enthalpy, and, ultimately, free energy calculations. The direct calculation method provided

172    above requires only empirical $C_P$ for data input, thus avoiding curve-fitting uncertainties or

173    human-induced bias. Therefore the utility of this method is, vast and has direct application

174    to fluid-rock interactions. , Specific examples including slab-subduction (i.e., Peacock, 1987),

175    hydrothermal or geothermal systems, and equilibrium speciation modeling. While the

176    mineral hematite was used as an illustrative example, this method has been applied to

177    diamond due to its use in high-temperature mantle research (e.g., Stachel et al., 2022) and to

178    quartz because of its ubiquity. In addition, we have applied this method to mineral

179    assemblages used in geothermometry, including galena-pyrite-sphalerite (Smith et al.,

180    1977), biotite-garnet (as pyrope and almandine) (Ferry and Spear, 1978), and muscovite-

181    biotite (e.g., Hoisch, 1989). The $C_p$ coefficients for almandine, diamond, muscovite, pyrite,

182    pyrope, quartz, and sphalerite have been calculated over at least two temperature domains

183    and are compared against tabulated values. These results are provided as Supplementary

184    Information. The method given above, however, can still be improved. Future work could

185    examine coefficient behavior by dividing temperature domains into smaller $\Delta T$ subsections.

186    Generation of $C_P$ coefficients from rref direct calculation for smaller temperature intervals is

187    expected to be more accurate than using coefficients under the conventional 'two-domain'

188    approach-especially for temperature ~900 to 1300 K (Interval #6 in Table 2 and Figure 2).

189    Finally, developing an understanding of the interesting local minimum at ~1300 K would

190    almost certainly prove fruitful.

# Acknowledgements

# References

197 Benisek, A., Kroll, H., and Dachs, E., 2012, The heat capacity of fayalite at high temperatures,
198        American Mineralogist, v. 97, p. 657-660

199 Ferry, J.M., and Spear, F.S., 1978, Experimental calibration of the partitioning of Fe and Mg
200        between biotite and garnet, Contributions to Mineralogy and Petrology, v. 66, p. 113-
201        117

202 Fuchs, S., Förster, H.J., Norden, B., Balling, N., Miele, R., Heckenbach, E. and Förster, A., 2021,
203        The thermal diffusivity of sedimentary rocks: Empirical validation of a physically
204        based α – φ relation. Journal of Geophysical Research: Solid Earth, 126,
205        e2020JB020595

206 Gamsjäger, E., and Wiessner, M., 2018, Low temperature heat capacities and thermodynamic
207        functions described by Debye-Einstein integrals, Monatshefte für Chemie - Chemical
208        Monthly, v. 149, p. 357-368

209    Guyot, F., Richet, P., Courtial, P., and Gillet, P., 1993, High-temperature heat capacity and
210          phase transitions of CaTiO$_3$ perovskite, Physics and Chemistry of Minerals, v. 20, p.
211          141-146

212    Hemingway, B.S., Robie, R.A., and Kittrick, J.A., 1978, Revised values for the Gibbs free energy
213          of formation of [Al(OH)$_{4\text{-aq}}$], diaspore, boehmite and bayerite at 298.15 K and 1 bar,
214          the thermodynamic properties of kaolinite to 800 K and 1 bar, and the heats of
215          solution of several gibbsite samples, Geochimica et Cosmochimica Acta, v. 42, p. 1533-
216          1543

217    Hemingway, B.S., 1990, Thermodynamic properties for bunsenite, NiO, magnetite, Fe$_3$O$_4$, and
218          hematite, Fe$_2$O$_3$, with comments on selected oxygen buffer reactions, American
219          Mineralogist, v. 75, p. 781-790

220    Hoisch, T.D., 1989, A muscovite-biotite geothermometer, American Mineralogist, v. 74, p.
221          565-572

222    Klemme, S., and van Miltenburg, J.C., 2003, Thermodynamic properties of hercynite
223          (FeAl$_2$O$_4$) based on adiabatic calorimetry at low temperatures, American
224          Mineralogist, v. 88, p. 68-72

225    Kong, Q., Siauw, T., and Bayen, A.M., 2021, Python Programming and Numerical Methods: A
226          Guide for Engineers and Scientists, Academic Press, London, pp. 456

227    Maier, C.G., and Kelley, K.K., 1932, An equation for the representation of high-temperature
228          heat content data, Journal of the American Chemical Society, v. 54, p. 3243-3246

229    Peacock, S.M., 1987, Thermal effects of metamorphic fluids in subduction zones, Geology, v.
230          15, p. 1057-1060

231    Robie, R.A., Hemingway, B.S., and Wilson, W.H., 1978, Low-temperature heat capacities and
232          entropies of feldspar glasses and of anorthite, American Mineralogist, v. 63, p. 109-
233          123

234    Robie, R.A., and Hemingway, B.S., 1995, Thermodynamic properties of minerals and related
235          substances at 298.15 K and 1 Bar (10$^5$ Pascals) pressure and at higher temperatures,
236          U.S. Geological Survey Bulletin 2131, U.S., Department of the Interior, Denver, pp. 461

237    Smith, J.W., Doolan, S., and McFarlane, E.F., 1977, A sulfur isotope geothermometer for the
238          trisulfide system galena-sphalerite-pyrite, Chemical Geology, v. 19, p. 83-90

239    Stachel, T., Cartigny, P., Chacko, T., and Pearson, D.G., 2022, Carbon and nitrogen in mantle-
240          derived diamonds, Reviews in Mineralogy and Geochemistry, v. 88, p. 809-875

241    Toulmin, P., III., and Barton, P.B., II., 1964, A thermodynamic study of pyrite and pyrrhotite,
242          Geochimica et Cosmochimica Acta, v. 28, p. 641-671

243    Ulain, G., Moro, D., and Valdré, G., 2020, Thermodynamic and thermoelastic properties of
244          wurtzite-ZnS by density function theory, American Mineralogist, v. 105, p. 1212-1222

245  Vassiliev, V.P., and Taldrik, A.F., 2021, Description of the heat capacity of solid phases by a
246        multiparameter family of functions, Journal of Alloys and Compounds, v. 872, 159682

247  Waples, D.W., and Waples, J.S., 2004, A review and evaluation of specific heat capacities of
248        rocks, minerals and subsurface fluids. Part 1: Minerals and nonporous rocks, Natural
249        Resources Research v. 13, p. 97-122

250  Xiong, Z., Liu, X., Shieh, S.R., Wang, S., Chang, L., Tang, J., Hong, X., Zhang, Z., and Wang, H.,
251        2016, Some thermodynamic properties of larnite ($\beta$-Ca$_2$SiO$_4$) constrained by high T/P
252        experiment and/or theoretical simulation, American Mineralogist, 101, p. 277-288.

253  **Figure and Table Captions**

254  Figure 1: Hematite C$_P$ coefficients across the two major temperature domains as found in
255  Hemingway (1990).  The low temperature domain represents the coefficients for T<950 K,
256  while the high temperature domain represents the coefficients for T>950 K.  Coefficients
257  calculated through rref methodology (400 to 800 K (for T<950 K) and 1000 to 1400 K (for
258  T>950 K) correspond to subintervals #2 and #6 in Table 1 respectively) are compared to
259  those reported in Robie and Hemingway (1995).  A) Coefficients A,B,C, and D.  B)  Coefficient
260  E.

261  Figure 2: Hematite heat capacity values as reported in Hemingway (1990) with
262  corresponding temperature intervals (as given in Table 1).  The numbered temperature
263  subintervals are those which were used to evaluate the polynomial coefficients reported in
264  Table 1 at each interval.  Red dots and blue triangles are the respective <950 K and >950 K
265  of the major 'two-domain' temperature intervals.  Black line indicates function discontinuity
266  at 950 K.

267  Table 1:  Heat capacity coefficients for hematite calculated at $\Delta T$ of ~400 K using rref and
268  C$_P$(T) found in Hemingway (1990).

269  **Tables**

270  **Table 1**

| T Interval (K-K) | Fig. 2 Interval # | Hematite Heat Capacity Coefficients | | | | |
|---|---|---|---|---|---|---|
| | | A | B | C | D | E |
| 298.15-700 | 1 | 841.57 | -0.65736 | 3.3946E-04 | -1.0901E+04 | 5.2795E+06 |
| 400-800 | 2 | 994.40 | -0.78862 | 3.9574E-04 | -1.3361E+04 | 7.4669E+06 |
| 500-900 | 3 | 1.1801E+03 | -0.92370 | 4.4462E-04 | -1.6606E+04 | 1.1139E+07 |
| 600-950 | 4 | 1.3253E+03 | -1.0102 | 4.7053E-04 | -1.9417E+04 | 1.5526E+07 |
| | | | | | | |
| 950-1300 | 5 | -402.36 | -9.0874E-03 | 5.7717E-05 | 1.7680E+04 | -5.6871E+07 |
| 1000-1400 | 6 | -1283.6 | 0.34356 | -1.3459E-05 | 3.8537E+04 | -1.1664E+08 |

| 1100-1500 | 7 | -579.09 | -0.10303 | 2.8004E-05 | 2.0480E+04 | -5.0923E+07 |
|-----------|---|---------|----------|------------|------------|-------------|
| 1200-1600 | 8 | -448.63 | 5.9654E-02 | 3.5304E-05 | 1.7089E+04 | 3.7975E+07 |
| 1300-1700 | 9 | 2.9410E+03 | -0.92811 | 1.8031E-04 | -7.6875E+04 | 3.9375E+08 |
| 1400-1800 | 10 | 88.544 | -5.8354E-02 | 4.6708E-05 | 416.67 | 6.2500E+07 |

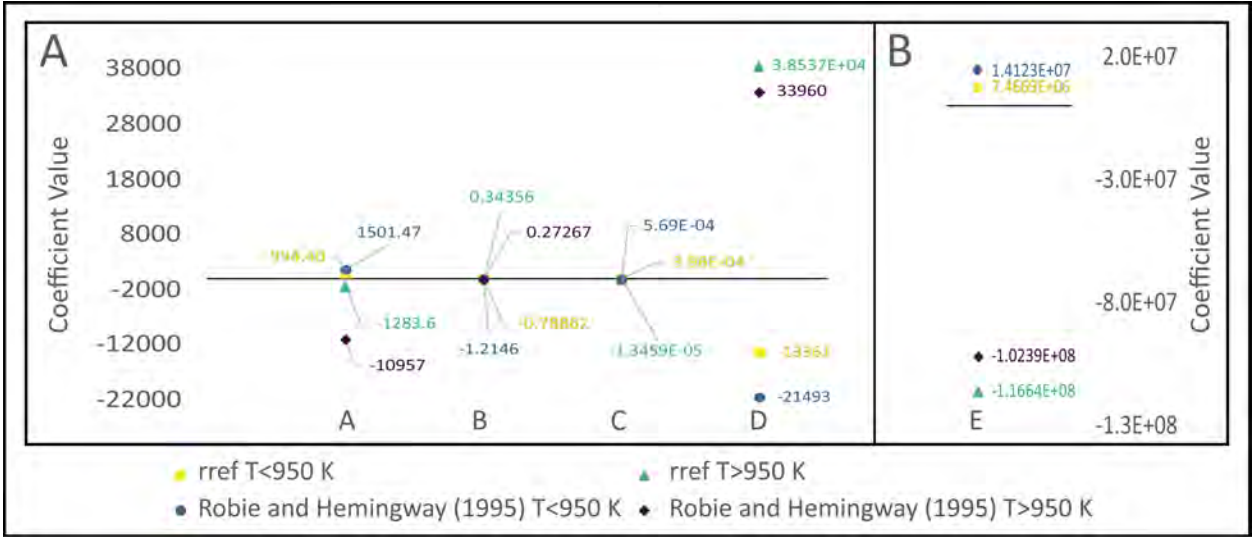271                                                            **Figures**

272    **Figure 1**



273

274    **Figure 2**

275